ULTIMATE STATE OF THIN-WALLED HOLLOW CIRCULAR STEEL COLUMNS SUBJECTED TO BI-DIRECTIONAL HORIZONTAL SEISMIC FORCES AND TRI-DIRECTIONAL SEISMIC MOMENTS

M. Assad. ALAMIRI [1*†], Yoshiaki. GOTO[2]

[1]*Department of Civil Engineering, Nagoya Institute of Technology, Japan*
[2]*Department of Civil Engineering, Nagoya Institute of Technology, Japan*

ABSTRACT

Torsional moment acts at the top of columns of bridge piers, when elevated curved girder bridges or elevated girder bridges supported by inverted L-shaped bridge piers are subjected to seismic accelerations. Therefore, to evaluate the safety of the bridge piers in the above types of bridges, it is essential to consider the effect of the torsional moment on piers. Herein, focusing on the effect of the torsional moment, versatile interaction surface expressed in terms of bi-directional horizontal seismic force and tri-directional seismic moment components is derived by the so-called pushover analysis to express the ultimate state of thin-walled hollow circular steel columns. The accuracy and validity of the derived ultimate interaction surface is examined by carrying out nonlinear dynamic response analysis on inverted L-shaped bridge pier models under variously factored bi-directional horizontal seismic acceleration components. As a result, it is observed that the derived ultimate interaction surface well predict the ultimate state of the pier models although it is a little conservative.

Keywords: Steel piers, Torsional moment, Limit State, Seismic design, Nonlinear Analysis.

1. INTRODUCTION

The elevated girder bridge piers are normally subjected to 3D components of seismic accelerations. However, our recent research (Goto and Ebisawa 2010) revealed that the coupling of two horizontal seismic acceleration components has a significant impact on the ultimate behaviors of elevated girder bridge piers. Therefore, to ensure their safety, it is essential to examine the ultimate behavior of bridge piers under bi-directional seismic accelerations and specify their ultimate state. For this purpose, authors (Obata and Goto 2007) first developed an accurate 3D loading system as well as a rigorous finite element nonlinear shell analysis (Goto et al. 2006). By the use of these tools, the ultimate behavior of thin-walled steel columns subjected to bi-directional horizontal seismic accelerations is extensively studied (Goto et al. 2006; Goto el at. 2009) both analytically and experimentally. Based on these studies, an interaction surface expressed in terms of bi-directional horizontal force components and bi-axial bending moment components acting at the top of thin-walled steel columns was derived to express the ultimate state of bridge piers (Goto el at. 2009; Goto and Ebisawa 2010). However, seismic accelerations induce torsional moment at the top of the columns of elevated curved girder bridge piers or the columns of inverted L-shaped bridge piers, as shown in Figure 1. Therefore, as a versatile interaction equation to predict the ultimate state of columns used for bridge piers, it is important to consider the effect of the torsional moment component in addition to that of bi-directional horizontal force components and bi-axial bending moment components. Gao et al. (2000) presented a formula to predict the ultimate states of inverted

* Corresponding author: Email: assad@kozo2.ace.nitech.ac.jp

† Presenter: Email: assad@kozo2.ace.nitech.ac.jp

L-shaped piers under out-of-plane horizontal loading where torsional moment acts at the top of the piers. However, this formula is only applicable to a specific case of the inverted L-shaped piers where an out-of-plane horizontal seismic force and a dead load act at a single point on the cross beam.

Herein, in order to derive the aforementioned versatile interaction equation of thin-walled circular steel columns used for bridge piers, the existing ultimate interaction surface (Goto and Ebisawa 2010) for the columns under bi-directional horizontal force components and bi-axial bending moment components is modified to take into account the effect of torsional moment component. The thin-walled circular steel columns considered herein have the radius-to-thickness parameter in the range of $0.04 \le R_t = (R/t)(\sigma_y / E)\sqrt{3(1-\nu^2)} \le 0.12$.

2. ULTIMATE STATE UNDER BI-DIRECTIONAL HORIZONTAL SEISMIC ACCELERATIONS

2.1. Ultimate State of Thin-walled Steel Columns

The conventional Japanese highway bridge design code (Japan Road Association 2012a) stipulates that the thin-walled steel column reaches its ultimate state at the limit point of the horizontal force vs. horizontal displacement curve. This criterion is reasonable both from theoretical and engineering viewpoints because the limit point is theoretically a transition point from stable to unstable state. Furthermore, the thin-walled columns used as bridge piers normally reach this point due to plastification together with the local buckling (Goto et al. 2006; Goto el at. 2009). This implies that the limit point is an initiation point of serious damage that may be considered as an ultimate state of thin-walled steel columns from engineering viewpoint. Under the seismic loads, even if a column temporarily falls into instability state, it can regain its stability after the major seismic acceleration is over. However, once column deforms beyond the limit point, the damage of column is likely to be evident. Herein, the initial transition point from stability state to instability state that is identified by the multi-dimensional elastic-plastic stability criterion (Hill 1958; Goto et al. 2009) is defined as the ultimate state of thin-walled steel columns under bi-directional horizontal force components, bi-axial bending moment components, and torsional moment component. As is well known, the static stability criterion cannot identify the occurrence of some types of dynamic instability phenomena. In these cases, however, if sway displacement increases large enough to inflict damages on columns, these columns will reach an instability state that can be identified by the static stability criterion.

2.2. Stability Criterion of Thin-walled Steel Columns under Bi-directional Horizontal Force, Bi-axial Bending Moment and Torsional Moment

The stability criterion of multi-dimensional elastic-plastic static theory (Hill 1958) generally classifies the equilibrium state of columns as stable, critical and unstable according to whether the 2nd order of work $\Delta^2 W$ given by equation (1) is positive, zero or negative, respectively.

In our previous research (Goto and Ebisawa 2010), the stability criterion was shown for the case where bi-directional horizontal force components $\left(F_x, F_y\right)$ and bi-axial bending moment components $\left(M_x, M_y\right)$ act at the top of columns. In the present case, the effect of torsional moment M_z has to be added. As a result, the 2nd order of work used for the stability criterion is expressed as

$$\Delta^2 W = (\Delta F_x \Delta u_x + \Delta F_y \Delta u_y + \Delta M_x \Delta \theta_x + \Delta M_y \Delta \theta_y + \Delta M_z \Delta \theta_z)/2 \quad (1)$$

where $(\Delta u_x, \Delta u_y)$ and $(\Delta\theta_x, \Delta\theta_y, \Delta\theta_z)$ denote arbitrary small incremental components of bi-directional horizontal displacement components and rotational components around 3 orthogonal coordinate axes (x, y, z) from an equilibrium state. $(\Delta F_x, \Delta F_y)$, $(\Delta M_x, \Delta M_y)$ and ΔM_z denote the resulting increments of bi-directional horizontal force components, bi-axial bending moment components and torsional moment component acting at the top of a column.

Theoretically, the stability of equilibrium state has to be examined by equation (1) for all the possible increments of displacement and rotation components. Practically, however, it is difficult to cover all the possible increments. Herein, as an acceptable alternative, $\Delta^2 W$ is examined following the response history of a pier (Goto et al. 2009). It must be noted that the zero-crossing point of $\Delta^2 W$ from positive to negative so evaluated yields only a sufficient condition for instability initiation point. However, considering that the safety check in the conventional seismic design is made on the basis of displacements or forces calculated following the response history of structures, the proposed evaluation method for $\Delta^2 W$ may be justified at least within the framework of the conventional design method.

3. ULTIMATE INTERACTION SURFACE UNDER BI-DIRECTIONAL HORIZONTAL FORCES, BI-AXIAL BENDING MOMENTS AND TORSIONAL MOMENT

3.1. Definition of Ultimate Interaction Surface

As an alternative method to identify the ultimate state of thin-walled steel columns, it will be convenient in practical seismic design to express the ultimate state in terms of response force components or response displacement components acting at the top of the columns. This is because these physical quantities are easily obtained by seismic response analysis. According to our previous research (Goto et al. 2009), the ultimate state of columns expressed by displacement components is strongly influenced by response history, whereas the ultimate state expressed by force components is less influenced. Therefore, authors proposed to use the mechanical quantities such as seismic force and moment components at the top of columns to express the ultimate state of columns of bridge piers subjected to bi-directional horizontal seismic accelerations and derived a versatile multi-dimensional interaction surface defined in terms of these force and bending moment components by employing pushover analysis (Goto and Ebisawa 2010). This multi-dimensional surface is referred to as an ultimate interaction surface. From numerical analysis together with shaking table test, it was confirmed that columns exhibit instability behavior after the response force components and moment components nearly touches the ultimate interaction surface (Goto et al. 2009; Goto and Ebisawa 2010).

Considering the accuracy and validity of the abovementioned ultimate interaction surface, the ultimate interaction surface of circular thin-walled steel columns with the effect of torsional moment is herein derived by modifying the existing ultimate interaction surface that considers the effect of bi-directional horizontal force components and bi-axial bending moment components (Goto and Ebisawa 2010).

3.2. Ultimate Interaction Surface under Bi-directional Horizontal Forces and Bi-axial Bending Moments

The existing ultimate interaction surface of thin-walled circular columns under bi-directional horizontal force and bi-axial bending moment components (Goto and Ebisawa 2010) is expressed as

$$\left(\frac{F_{xu} + M_{yu}/h^{eq}}{\overline{F}^{P}_{xu}}\right)^2 + \left(\frac{F_{yu} - M_{xu}/h^{eq}}{\overline{F}^{P}_{yu}}\right)^2 = 1 \tag{2}$$

where $\left(F_{xu}, F_{yu}\right)$ and $\left(M_{xu}, M_{yu}\right)$ are the force and bending moment components at the top of a column when the column reaches the ultimate state. h^{eq} is the equivalent height. In the numerical analysis, thin-walled circular columns are observed to reach their ultimate state when the bending moment at the height of $(h-h^{eq})$ becomes equal to the bending moment capacity of thin-walled cross section under constant compressive force P. $\overline{F}_{xu}^{P}$ and $\overline{F}_{yu}^{P}$ are the maximum horizontal forces calculated by the unidirectional pushover analyses in the x and y directions. If the columns are fabricated within an allowable geometrical tolerance specified in Japanese design code (Japan Road Association 2012b), $\overline{F}_{xu}^{P}$ and $\overline{F}_{yu}^{P}$ can be considered to be approximately coincident with the maximum horizontal force $\overline{F}_{u}^{P}$ for ideal piers without geometrical imperfection. Therefore, $\overline{F}_{xu}^{P} \approx \overline{F}_{yu}^{P} \approx \overline{F}_{u}^{P}$ is herein assumed. Empirically obtained formulas to calculate h^{eq} and $\overline{F}_{u}^{P}$ are shown elsewhere (Goto and Ebisawa 2010).

3.3. Ultimate Interaction Surface under Bi-directional Horizontal Forces, Bi-axial Bending Moments and Torsional Moment

Considering the circular cross section of a column, the shape of the interaction surface is rotational symmetry in terms of the axis that denotes the magnitude of the torsional moment. Therefore, the ultimate interaction surface of a thin-walled circular column under bi-directional horizontal forces, bi-axial bending moments and torsional moment shown in Figure 1 (b) can be expressed as

$$\left\{\left(\frac{F_{xu}+M_{yu}/h^{eq}}{\overline{F}_{u}^{P}}\right)^{2}+\left(\frac{F_{yu}-M_{xu}/h^{eq}}{\overline{F}_{u}^{P}}\right)^{2}\right\}^{\alpha}+\left(\frac{M_{zu}}{\overline{M}_{zu}^{P}}\right)^{\beta}=1 \tag{3}$$

where $\left(F_{xu}, F_{yu}\right)$, $\left(M_{xu}, M_{yu}\right)$ and M_{zu} are the bi-directional force, bi-axial bending moment and torsional moment components acting at the top of a column when the column reaches the ultimate state. $\overline{M}_{zu}^{P}$ denotes the maximum torsional moment obtained by monotonically increasing twisting rotation θ_z around z axis at the top of a column under constant compressive force P. In order to stabilize the numerical analysis to calculate $\overline{M}_{zu}^{P}$, the small geometrical initial imperfection with $\Delta R/R = 1/500$ shown in Figure 3 (c) or (d) is considered. $\Delta R/R$=1/500 is specified by Japanese design code as an allowable tolerance (Japan Road Association 2012b). α and β are the curve-fitting constants. These constants are determined so that the interaction surface best fits the ultimate points obtained by pushover analyses that are carried out into various directions as shown in Figure 2. These limit points are identified by the stability criterion, equation (1).

For the ease of expression, total equivalent horizontal force components $\left(F_x^{eq}, F_y^{eq}\right)$ defined as $F_x^{eq} = \left(F_x + M_y/h^{eq}\right)$ and $F_y^{eq} = \left(F_y - M_x/h^{eq}\right)$ are hereinafter used.

4. VERIFICATION OF ULTIMATE INTERACTION SURFACE UNDER SEISMIC ACCELALATIONS

4.1. Test Models

The validity of the ultimate interaction surface given by equation (3) is examined by computing the ultimate seismic behavior of thin-walled circular bridge piers numerically. An inverted L-shaped pier shown in Figure 3 is adopted as a bridge pier model so that the seismic torsional moment acts at the top of the columns in addition to the bi-directional seismic force and bi-axial

bending moment components. In this model, elastic diaphragms with the thickness of $12mm$ are assumed to be installed to the internal hollow space of the circular column with an equal interval of $d = 3R$. In the pier model, the column is discretized by four-node shell elements (S4R), while the cross beam with a concentrated mass of eccentric distance e is expressed by rigid beam element (MPC). Two types of the inverted L-shaped pier models used in the analysis are summarized in Table 1. In these models, two kinds of eccentricity ratios are adopted. However, the radius-to-thickness ratio parameter R_t, slenderness ratio parameter $\overline{\lambda}$, diaphragm interval ratio $d/(2R)$ and axial force ratio P/P_y are the same. Most of these quantities are determined referring to the model used by Gao et al (2000). For the ease of obtaining the convergence of solution, two kinds of cross sectional geometrical imperfection modes with magnitude of $\Delta R/R = 1/500$ illustrated in Figure 3(c) and (d) are considered for the respective column models. The curve-fitting constants of the ultimate interaction surface expressed by equation (3) are determined for the above column model as $\alpha = 0.569$ and $\beta = 4.371$.

To calculate the ultimate seismic behavior of the pier models, the geometrically and materially nonlinear dynamic shell analysis with the three-surface cyclic metal plasticity constitutive model is carried out by the general purpose finite element software ABAQUS (2007). As input bi-directional horizontal seismic acceleration waves, variously factored NS and EW components of JRT observed during the 1995 Kobe earthquake are simultaneously applied to the directions of x and y axes, respectively, defined in terms of the inverted L-shaped pier model shown in Figure 1. The factored bi-directional waves used for dynamic response analysis are created by multiplying the magnification factor C ranging from 0.1 to 1.0.

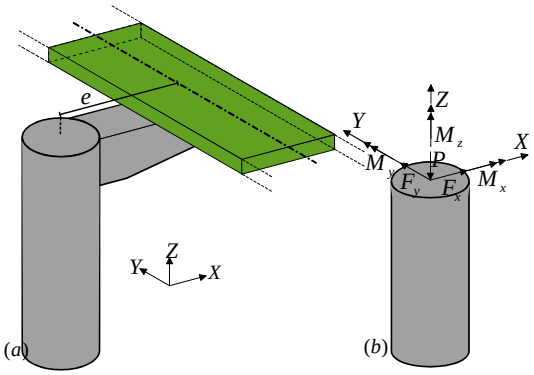

Figure 1: Seismic inertial forces acting at the top of inverted L-shaped circular pier

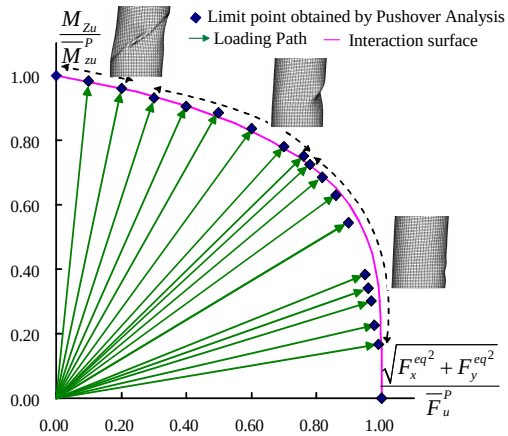

Figure 2: Loading path to derive the ultimate interaction surface

Table 1: Geometrical Properties of Pier Models

Pier model	P2-e1	P2-e2
e/h	0.1	0.2

$R = 1000(mm)$; $t = 34(mm)$; $h = 8520(mm)$; $h_s = 200(mm)$;
$Mass = 1000(ton)$; $\Delta R/R = \pm 1/500$; $d = 3R$;
$P/P_y = 0.15$; $R_t = (R/t)(\sigma_y/E)\sqrt{3(1-\upsilon^2)} = 0.074$;
$\overline{\lambda} = \sqrt{\sigma_y A/P_{cr}} = 0.3$

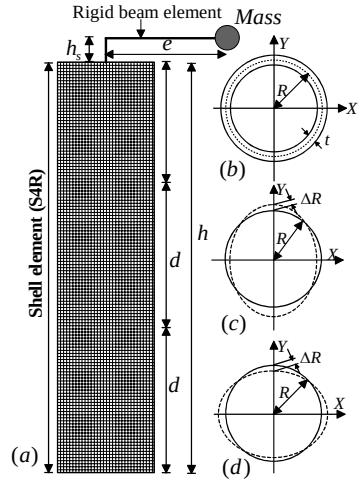

Figure 3: Analytical model of pier

(a) Inverted L-shaped circular pier (b) Ideal circular cross section (c and d) Circular cross section with initial imperfection

4.2. Validity of Ultimate Interaction Surface under Bi-directional Seismic Accelerations

First, it is investigated in terms of the seismic response inertia force components $\left(F_x, F_y\right)$ and moment components $\left(M_x, M_y, M_z\right)$ at the top of columns how columns of the inverted L-shaped piers reach instability state. For this purpose, trajectories of the response components of $\left(F_x^{eq}/\overline{F}_u^P,\ F_y^{eq}/\overline{F}_u^P,\ M_z/\overline{M}_{zu}^P\right)$ are expressed in comparison with the ultimate interaction surface. As an example, the trajectories are illustrated in Figure 4 for the column of pier model P2-e2 under JRT×0.1 and JRT×1.0. In this figure, in order to show the 3D trajectories, the projections of the trajectories on $\left(\sqrt{F_x^{eq^2}+F_y^{eq^2}}/\overline{F}_u^P,\ M_z/\overline{M}_{zu}^P\right)$ and $\left(\dfrac{F_{xu}^{eq}/\overline{F}_u^P}{\left(1-\left(M_z/\overline{M}_{zu}^P\right)^\beta\right)^{1/(2\alpha)}}, \dfrac{F_{yu}^{eq}/\overline{F}_u^P}{\left(1-\left(M_z/\overline{M}_{zu}^P\right)^\beta\right)^{1/(2\alpha)}}\right)$ planes are shown in Figure 4. In Figure 4, the notations such as $\overline{F}_{xu}^{eq}=F_{xu}^{eq}\Big/\left(1-\left(M_z/\overline{M}_{zu}^P\right)^\beta\right)^{1/(2\alpha)}$ and $\overline{F}_{yu}^{eq}=F_{yu}^{eq}\Big/\left(1-\left(M_z/\overline{M}_{zu}^P\right)^\beta\right)^{1/(2\alpha)}$ are used to simplify the expression.

As can be seen from Figure 4, when JRT×0.1 wave with small acceleration magnitude is applied, the trajectory is located inside the ultimate interaction surface and the column is stable. However, when JRT×1.0 wave with larger acceleration magnitude is applied, the outermost trajectory comes very close to the ultimate interaction surface and proceeds along the interaction surface, instead of penetrating the surface straightly. When the trajectory almost touches the ultimate interaction surface, the pier becomes unstable afterwards. This behavior is almost the same as that of a column subjected to bi-directional horizontal seismic force components $\left(F_x, F_y\right)$, (Goto et al. 2009). Therefore, the validity of the ultimate interaction surface can be confirmed for the present case where the 3D seismic moment components $\left(M_x, M_y, M_z\right)$ in addition to the bidirectional horizontal seismic force components $\left(F_x, F_y\right)$ acts at the top of the column.

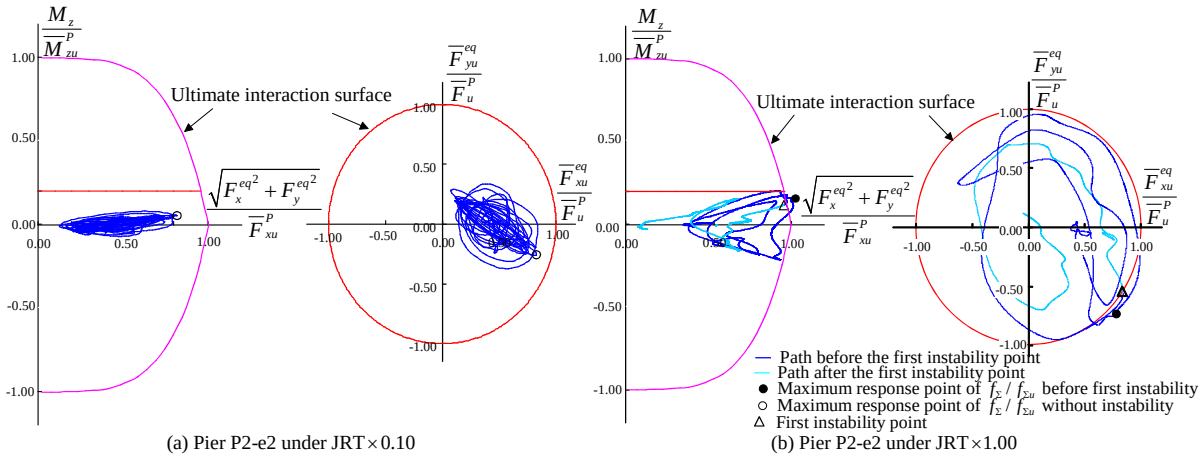

(a) Pier P2-e2 under JRT×0.10 (b) Pier P2-e2 under JRT×1.00

Figure 4: Trajectories of response force components and ultimate interaction surface

Second, the accuracy of the interaction surface is examined for two types of inverted L-shaped pier models P2-e1 and P2-e2 with the different eccentricity ratios of $e/h=0.1$ and 0.2. These pier models are assumed to have two types of initial geometrical imperfection modes illustrated in

Figure 3(c) and (d) with magnitude of $\Delta R/R = 1/500$. The ultimate behaviors of these piers are calculated by applying bi-directional horizontal components of variously factored JRT waves. Magnification factors considered, herein, are $C = 0.1$, 0.4, 0.7, 0.8, 0.9 and 1.0. The accuracy of the ultimate interaction surface (equation (3)) is examined for the cases when instability occurs by comparing the maximum response points with the ultimate interaction surface. For this purpose, the quantity $f_\Sigma / f_{\Sigma u}$ defined by equation (4) is used.

$$\frac{f_\Sigma}{f_{\Sigma u}} = \sqrt{\left(\frac{F_x^{eq}}{\overline{F}_u^P}\right)^2 + \left(\frac{F_y^{eq}}{\overline{F}_u^P}\right)^2 + \left(\frac{M_z}{\overline{M}_{zu}^P}\right)^2} \Bigg/ \sqrt{\left(\frac{F_{xu}^{eq}}{\overline{F}_u^P}\right)^2 + \left(\frac{F_{yu}^{eq}}{\overline{F}_u^P}\right)^2 + \left(\frac{M_{zu}}{\overline{M}_{zu}^P}\right)^2} \tag{4}$$

where F_{xu}^{eq}, F_{yu}^{eq} and M_{zu} are the quantities on the point of the ultimate interaction surface where the extended response vector $\left(F_x^{eq}/\overline{F}_u^P,\ F_y^{eq}/\overline{F}_u^P,\ M_z/\overline{M}_{zu}^P\right)$ intersects. f_Σ and $f_{\Sigma u}$ are schematically shown in Figure 5. For the cases when instability occurs, the maximum response points of $f_\Sigma / f_{\Sigma u}$ before the occurrence of the first instability are marked by filled circles in the space defined in terms of $\left(F_x^{eq}/\overline{F}_u^P,\ F_y^{eq}/\overline{F}_u^P,\ M_z/\overline{M}_{zu}^P\right)$ coordinates. On the other hand, when instability does not occur during the whole response history, the maximum response points of $f_\Sigma / f_{\Sigma u}$ are similarly marked by empty circles. The 3D distribution of the aforementioned maximum response points are expressed by the projections of these points on $\left(\sqrt{F_x^{eq2} + F_y^{eq2}}/\overline{F}_u^P,\ M_z/\overline{M}_{zu}^P\right)$ plane and $\left(\overline{F}_{xu}^{eq}\Big/\overline{F}_u^P, \overline{F}_{yu}^{eq}\Big/\overline{F}_u^P\right)$ plane are shown in Figure 6. From Figure 6, it is observed that all the filled circles are located very close to the interaction surface and the empty circles are inside the interaction surface. Therefore, the interaction surface expressed by equation (3) well approximates in a conservative manner the ultimate states of columns under the coupling of the seismic response inertia force components $\left(F_x, F_y\right)$ and moment components $\left(M_x, M_y, M_z\right)$ at their top. However, as can be seen from Figure 6, the response torsional moment ratio $M_z\Big/\overline{M}_{zu}^P$ is less than 0.2. In this range, the effect of the torsional moment on the ultimate behavior of columns is too small to verify the accuracy of the interaction surface in wider range. Therefore, it will be necessary to use inverted L-shaped pier models with larger eccentricity ratios that exceed 0.2 in order to examine the accuracy of the interaction surface extensively, although the piers with the eccentricity ratio $e/h \geq 0.4$ are not common in practice.

5. SUMMARY AND CONCLUSION

In the view of the importance to ensure the safety of thin-walled hollow circular steel columns under torsional moment in addition to the bi-directional horizontal seismic force and bi-axial bending moment components, a versatile interaction surface is derived by the so-called pushover analysis to specify the ultimate state of thin-walled bridge piers. This ultimate interaction surface is herein expressed in terms of the torsional moment component together with the bi-directional horizontal force components and the bi-axial bending moment components acting at the top of the column. The validity and accuracy of this ultimate interaction surface is examined by carrying out nonlinear dynamic response analysis on inverted L-shaped bridge pier models under variously factored bi-directional horizontal seismic acceleration components. As a result, it is demonstrated that the derived ultimate interaction surface well predicts the ultimate state of the pier models although it is a little conservative. However, the response torsional moment ratio $M_z/\overline{M}_{zu}^P$ that

acts on the column of the inverted L-shaped pier models is a little too small to verify the accuracy of the interaction surface in a wider range. Therefore, in order to examine the accuracy of the interaction surface more extensively, it will be necessary to use inverted L-shaped pier models with extremely larger eccentricity ratios, although such piers are not common in practice.

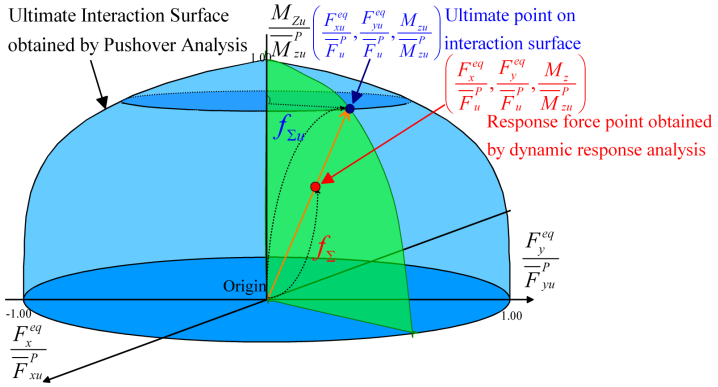

Figure 5: Schematic explanation for f_{Σ} and $f_{\Sigma u}$

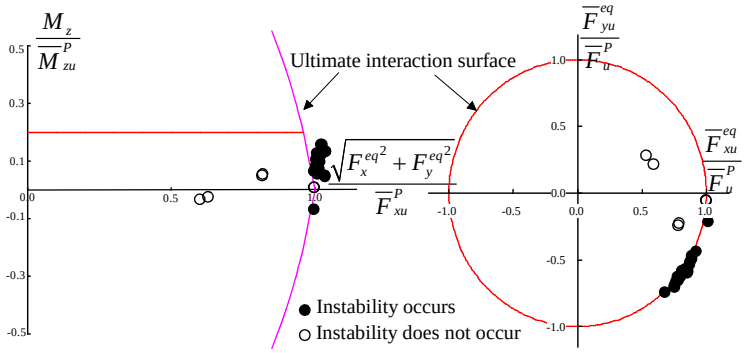

Figure 6: Maximum response points and ultimate interaction surface on $\left(\sqrt{F_x^{eq2}+F_y^{eq2}}\Big/\overline{F}_u^P, M_z\Big/\overline{M}_{zu}^P\right)$ and $\left(\overline{F}_{xu}^{eq}\Big/\overline{F}_u^P, \overline{F}_{yu}^{eq}\Big/\overline{F}_u^P\right)$ planes

REFERENCES

ABAQUS/ Standard 6.7 User's Manual, (2007). Hibbit Karlsson, and Sorensen. Inc.

Hill R. (1958). A General Theory of Uniqueness and Stability in Elastic – Plastic Solids. Journal of the Mechanics and Physics of Solids, 6, pp. 236-249.

Gao Shengbin, Usami Tsutomu, and Ge Hanbin (2000). Eccentrically Loaded Steel Columns under Cyclic Out-of-Plane Loading. Journal of Structural Engineering. 126(8), pp. 974-981.

Goto Yoshiaki and Ebisawa Takemasa (2010). Ultimate State of Thin-Walled Stiffened Square Steel Bridge Piers Subjected to Bi-directional Horizontal Seismic Forces and Bi-directional Directional Seismic Moments. Proceeding Ninth Pacific Structural Steel Conference, Beijing, pp. 1222-1229.

Goto Yoshiaki, Jiang Kunsheng, and Obata Makoto (2006). Stability and Ductility of Thin-Walled Circular Steel Columns under Cyclic Bidirectional Loading. Journal of Structural Engineering. 132(10), pp. 1621-1631.

Goto Yoshiaki, Muraki Masayuki, and Obata Makoto (2009). Ultimate State of Thin-Walled Circular Steel Columns under Bidirectional Seismic Accelerations. Journal of Structural Engineering. 135(12), pp. 1481-1490.

Japan Road Association (2012a). Specifications for Highway Bridges. Part V. Seismic Design, Tokyo, Japan.

Japan Road Association (2012b). Specifications for Highway Bridges. Parts I and II. Common and Steel Bridges, Tokyo, Japan. (In Japanese)

Obata Makoto and Goto Yoshiaki (2007). Development of Multidirectional Structural Pseudo dynamic test. Journal of Structural Engineering. 133(5), pp. 638-645.